Theoretical reinvestigation of high-spin spectroscopy of ^{164}Er

Yang Sun[*]

Department of Physics and Astronomy, University of Tennessee, Knoxville, Tennessee 37996

Kenji Hara[†]

Physik-Department, Technische Universität München, D-85747 Garching bei München, Germany
(Received 20 January 1998)

Motivated by the recent high-spin data [1], we reinvestigate the structure of various bands in the nucleus ^{164}Er in terms of the projected shell model, which describes all the bands by a single shell-model diagonalization. In the present work, it is found that an appropriate modification of the standard Nilsson (spin-orbit) parameters in the $N=5$ proton shell is necessary in order to correctly describe both the yrast and the negative parity bands. With the same Hamiltonian, there are discrepancies to the data for some sidebands. To cure them, we would need an investigation of a larger scope than the present one. [S0556-2813(98)06006-3]

PACS number(s): 21.60.Cs, 21.10.Re, 23.20.Lv, 27.70.+q

I. INTRODUCTION

The study of nuclear high-spin spectroscopy began in the early 1970s when the backbending in the moment of inertia was discovered in some well-deformed nuclei [2–4]. Since then, the high-spin study has been a very active research field in nuclear structure physics. In recent years, with rapid development and deployment of high performance detectors and accelerators, there has been a proliferation of measurements from year to year, with greater and greater accuracy and with higher and higher spins. These facilities are able to detect extremely narrow γ-ray widths, from which intricate and delicate high-spin phenomena have been discovered. Hence, one has expected that this field of research would be soon confronted with ever expanding sets of highly accurate high-spin data.

For the interpretation of these new data, it is required for a theoretical model to be able to well describe not only the yrast band but also many sidebands. Thus, the high-spin data may be used as a crucial test for the existing models. The well-deformed nucleus ^{164}Er is one of the earliest known examples in the rare-earth region [5]. In the past, it served as a testing ground for theories describing the backbending phenomenon. Also, it was one of the early examples with several sidebands in addition to the yrast band [6].

In a very recent experimental work [1], several known rotational bands in this nucleus have been extended considerably to higher spins and a new four-quasiparticle band has been established. In particular, we notice that the new data indicate a clear plateau behavior in the moment of inertia at higher spins in the yrast and the negative parity bands.

In our early systematic study of yrast bands of even-even rare-earth nuclei by using the projected shell model (PSM) [7], we predicted a second backbending in the moment of inertia in ^{164}Er at spin $I=26$. This prediction in the PSM was a consequence of the calculations which reasonably well reproduced all the high-spin data known at that time. However, since this prediction of the second backbending is not sup-

ported by the new data, we feel it necessary to find out the source of the discrepancy. As another interest of the present paper, it will be tested whether or not the whole set of the new data, including several sidebands up to very high spins, can be reproduced in the same PSM framework.

There has been a series of publications by using the PSM and, since an extensive review article containing a detailed description and many applications of the model (see Ref. [8], and references cited therein) exists, we shall not go into any detailed explanation of the model except for the following short account. The PSM closely follows the shell-model philosophy and is, in fact, a shell model truncated in a deformed basis. It proceeds as follows: first, the basis truncation is done in the multiquasiparticle (qp) basis by selecting low-lying states based on the Nilsson + BCS representation; then, the rotational symmetry (and the number conservation, if necessary) is restored for these deformed multi-qp states by the projection method to form a spherical (many-body) basis in the laboratory frame; finally, the Hamiltonian is diagonalized in this projected basis. The truncation achieved in this way is very efficient. In fact, quite satisfactory results can be obtained by choosing only a few orbitals near the Fermi surface since the deformed quasiparticle basis already contains most of important (pairing and quadrupole) correlations.

Deformation parameters in the Nilsson model are well studied quantities, so that we know exactly where the optimal basis is. In this paper, as in all other publications of the PSM, we take the deformation parameters from the literature. For ^{164}Er, we use $\varepsilon_2=0.258$ and $\varepsilon_4=0.001$ taken from Ref. [9]. This means that, instead of zero deformation in which the spherical shell model is based, we start from a nonzero deformation to build our shell-model basis. All the states within one nucleus will be obtained from the diagonalization in this (projected) shell-model basis without individually changing the deformation parameter for each band and spin. The relation of the input deformation parameter to the two-body interaction employed will be described below. There is a self-consistency relation between them, see Ref. [8].

The spin-orbit force parameters (or Nilsson parameters), κ and μ, appearing in the Nilsson model are essential in

*Electronic address: yangsun@utknp3.phys.utk.edu

†Electronic address: Kenji.Hara@physik.tu-muenchen.de

reproducing correct shell filling. They are important not only for odd mass and odd-odd nuclei but also for the excited configurations in even-even nuclei as we shall see in the present paper. In the calculations for rare-earth nuclei, we usually use the compilation made by Nilsson *et al.* [10] which was adjusted to the rare-earth region (*A* dependent). This is what we adopt in the present calculations allowing a slight modification if necessary. We mention that there are other compilations. Bengtsson and Ragnarsson [11] refitted these parameters to the experimental data which were available about 10 years ago. Their κ and μ are different for different major shells (*N* dependent) without explicit mass dependence, whose μ values for the proton $N=5$ and 6 were later revised by Zhang, Larabee, and Riedinger [12]. Seo [13] introduced *N*- and *l*-dependent κ and μ for a broad range of mass region with smaller number of parameters. However, for the PSM, we found that these compilations are not quite satisfactory at least for the present problem. It might depend on the models one uses.

The set of multi-qp states $\{|\Phi_\kappa\rangle\}$, which we want to take into account in the shell-model configuration space by projecting onto a good angular momentum *I*, is selected as

$$|0\rangle, \quad a^\dagger_{\nu_1} a^\dagger_{\nu_2}|0\rangle, \quad a^\dagger_{\pi_1} a^\dagger_{\pi_2}|0\rangle, \quad a^\dagger_{\nu_1} a^\dagger_{\nu_2} a^\dagger_{\pi_1} a^\dagger_{\pi_2}|0\rangle, \quad (1)$$

where $a^\dagger$'s are the qp creation operators and ν's (π's) denote the neutron (proton) Nilsson quantum numbers which run over properly selected (low-lying) orbitals. We have discarded configurations that contain three or more like-nucleon quasiparticles because they have higher excitation energies due to mutual blocking of levels and thus affect the results little in the energy (and the spin) range that interests us. This restriction can be released if necessary. Note that the index 1 and 2 in Eq. (1) are general. For example, a 2-qp state can be of positive parity if both quasiparticles 1 and 2 are from the same major shell; it can also be of negative parity if two quasiparticles are from two neighboring major shells. Positive and negative parity states span the whole configuration space with the corresponding matrix in a block-diagonal form classified by the parity.

In the present work, as in the usual PSM calculations, we use the Hamiltonian [8]

$$\hat{H} = \hat{H}_0 - \frac{1}{2}\chi \sum_\mu \hat{Q}^\dagger_\mu \hat{Q}_\mu - G_M \hat{P}^\dagger \hat{P} - G_Q \sum_\mu \hat{P}^\dagger_\mu \hat{P}_\mu, \quad (2)$$

where $\hat{H}_0$ is the spherical single-particle Hamiltonian which, in particular, contains a proper spin-orbit force. The second term in the Hamiltonian is the quadrupole-quadrupole interaction and the last two terms the monopole and quadrupole pairing interactions, respectively. The interaction strengths are determined as follows: the quadrupole interaction strength χ is adjusted such that the known (input) quadrupole deformation ε_2 is obtained as a result of the self-consistent mean-field calculations [8]. The monopole pairing strength G_M is of a standard form and is taken to be $G_M = [21.24 \mp 13.86(N-Z)/A]/A$, with ''−'' for neutrons and ''+'' for protons, which more or less reproduces the observed odd-even mass differences in this mass region. This choice of G_M is appropriate for the single-particle space employed in the
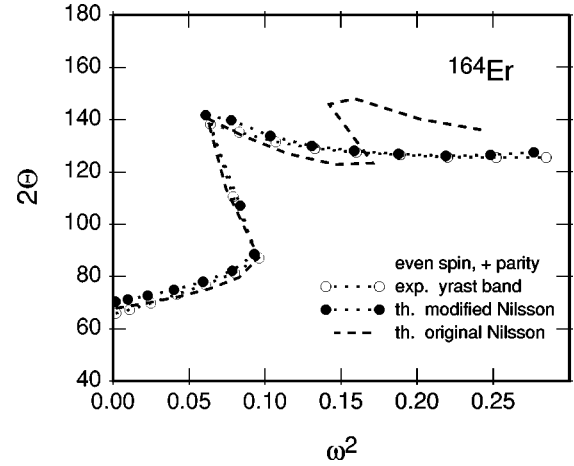
FIG. 1. Backbending plot for the yrast band (labeled as the *g* band and AB in Ref. [1]) in ^{164}Er. The new experimental data [1] are compared with two theoretical calculations which differ in the Nilsson parameters for the $N=5$ proton shell. Moment of inertia is defined as $\Theta = (2I-1)/2\omega$ (MeV^{-1}), while rotational frequency as $\omega = [E(I)-E(I-2)]/2$ (MeV). The same definitions will be used in Figs. 3 and 4.

PSM, where three major shells are used for each type of nucleons, i.e., $N=4,5,6$ for neutrons and $N=3,4,5$ for protons. The quadrupole pairing strength G_Q is assumed to be proportional to G_M, the proportionality constant being fixed to be 0.16 in the present work. These interaction strengths are consistent with those used in the previous works for the same mass region [8].

II. THE YRAST BAND

In Fig. 1, we show the backbending plot for the yrast band of ^{164}Er. Two theoretical results are presented together with the new experimental data [1]. The experimental yrast band is plotted by taking the lower state at each spin after comparing the ground band (*g* band) and the *s* band (labeled as AB in Ref. [1]). Under the same condition [the same input deformation parameter, interaction strengths in Eq. (2) and truncation in the configuration space], we compare the two theoretical results. In both of them, the experimental data are very nicely reproduced until $\omega^2 \approx 0.15$. However, in one of these results (dashed line in Fig. 1), which we first presented in one of our earlier papers [7], the theoretical curve exhibits a second backbending at $\omega^2 \approx 0.16$ (corresponding to spin *I* $=26$). Obviously, this prediction is not supported by the new data [1] which shows a plateau after the first backbending. On the other hand, the second theoretical result (filled circles in Fig. 1 obtained by modifying the standard Nilsson parameters) reproduces nicely the new data for the entire region of the rotational frequency.

One of the motivations of the present work is to find out why the second backbending has occurred in our earlier calculation. For this purpose, the band diagram [8] is the most appropriate tool as it shows the detailed behavior of various bands as a function of spin.

The band diagrams corresponding to the above-mentioned two theoretical results are shown in Fig. 2. In these plots, filled circles represent the results for the yrast states obtained after the band-mixing, i.e., after the shell-model diagonaliza-
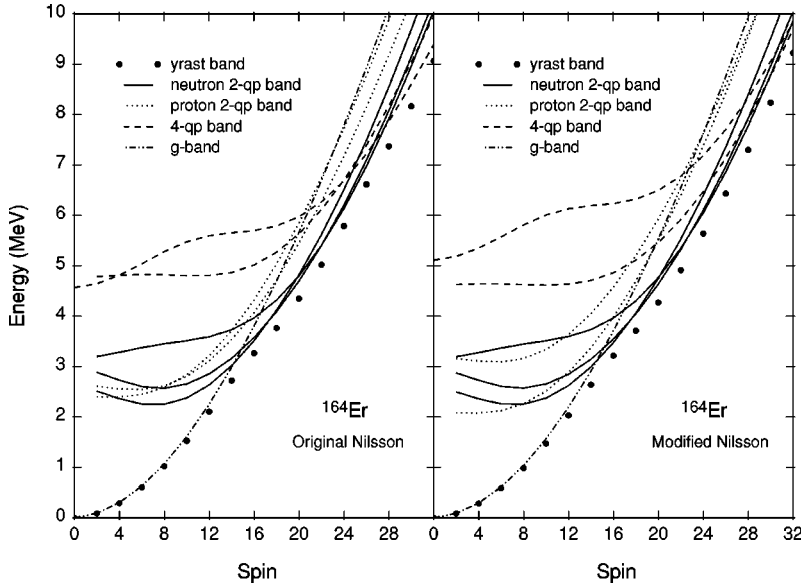
FIG. 2. Band diagram for the positive parity states in ^{164}Er. Only even spin states are plotted. The left figure (a) uses the original Nilsson parameters while the right figure (b) uses the modified ones for the proton $N=5$ shell.

tion. It can be seen from both Figs. 2(a) and 2(b) that the yrast band first smoothly follows the g band until spin $I=14$. This behavior is suddenly interrupted at this spin by a sharp band crossing with a neutron 2-qp band (showing the first backbending in the moment of inertia at $\omega^2 \approx 0.09$ in Fig. 1). Among many others, three neutron 2-qp bands are selected and shown in the band diagrams Figs. 2(a) and 2(b). These bands are built upon neutron 2-qp states from the $i_{13/2}$ subshell and are important for the yrast band evolution. Their configurations are (from the lowest to the highest at spin $I=2$): $[\frac{5}{2}^+,-\frac{7}{2}^+]K^\pi=-1^+$, $[-\frac{3}{2}^+,\frac{5}{2}^+]K^\pi=+1^+$ and $[\frac{1}{2}^+,\frac{5}{2}^+]K^\pi=2^+$. There are also two proton 2-qp bands built upon proton 2-qp states from the subshell $h_{11/2}$ with the configurations: $[-\frac{7}{2}^-,\frac{9}{2}^-]K^\pi=+1^+$ [lying slightly lower in Fig. 2(a)] and $[\frac{5}{2}^-,-\frac{7}{2}^-]K^\pi=-1^+$.

In Fig. 2(a), the next sharp band crossing is seen at the spin $I=26$, where a 4-qp state $(\nu i_{13/2}[-\frac{3}{2}^+,\frac{5}{2}^+]$ $\oplus \pi h_{11/2}[\frac{5}{2}^-,-\frac{7}{2}^-]K^\pi=0^+$, starting from $I=0$) crosses the neutron 2-qp bands. This sharp crossing is the source of our (wrongly) predicted second backbending of the yrast band. Another lower-lying 4-qp state $(\nu i_{13/2}[-\frac{3}{2}^+,\frac{5}{2}^+]$ $\oplus \pi h_{11/2}[-\frac{7}{2}^-,\frac{9}{2}^-]K^\pi=2^+$, starting from $I=2$) approaches and crosses the neutron 2-qp states in a very gentle way. However, this 4-qp band lies higher and thus does not enter into the yrast region.

It is clear that the wrong prediction of the second backbending can be avoided if the position of the 4-qp band with $K=0$ is shifted higher so that it will not sharply dive into the yrast line. The relative positions of various excited bands in a nucleus are sensitive to the deformed single-particle energies as determined by the Nilsson diagram. Since a 4-qp state consists of a neutron 2-qp and a proton 2-qp state, the position of a 4-qp band can be raised if either the neutron 2-qp or the proton 2-qp state is higher, or both. Because of the fact that the first backbending is reproduced rather well, which requires the right position of the neutron 2-qp states, it is reasonable to adjust the position of the proton quasiparticles in order to bring the 4-qp band to a right place.

Based on this consideration, we have modified the Nils-son parameters κ and μ for the $N=5$ proton shell (which contains the $h_{11/2}$ subshell) by simply multiplying a factor of 1.1, namely we have increased these parameters by 10% in order to shift the 4-qp state in question to a desired position. The resulting backbending plot is denoted as "modified Nilsson" in Fig. 1. The effect of this modification can be clearly seen in Fig. 2(b). The proton Fermi energy now lies between the Nilsson levels $K=\frac{7}{2}$ and $\frac{9}{2}$ and thus the proton 2-qp band $[-\frac{7}{2}^-,\frac{9}{2}^-]K^\pi=+1^+$ is shifted lower and the band $[\frac{5}{2}^-,-\frac{7}{2}^-]K^\pi=-1^+$ much higher. Due to this modification, the first 4-qp band which crosses the neutron 2-qp band is the one with $\nu i_{13/2}[-\frac{3}{2}^+,\frac{5}{2}^+]$ $\oplus \pi h_{11/2}[-\frac{7}{2}^-,\frac{9}{2}^-]K^\pi=2^+$. The crossing angle is rather small and thus nothing drastic can happen around the crossing spin. In fact, the perfect agreement with data in Fig. 1 (filled circles vs open circles) is achieved after this modification in the Nilsson parameters.

This might pose an interesting question about the "correctness" of the (proton) Nilsson diagram which serves as the standard basis for the structure calculations. The parameters used to generate the Nilsson diagram in the present paper were fitted nearly 30 years ago [10] when not many accurate and systematic high-spin data were available. The Nilsson parameters for the higher proton shells seem to be rather problematic and we feel that more intensive studies of the proton spin-orbit force have to be done. In this connection, we recall that, in our review article [8], where a systematic calculation is done for many different kinds of rare-earth nuclei, the theory agreed quite satisfactorily with data for even-even and odd-neutron systems but less satisfactorily for odd-proton and odd-odd systems where correct proton Nilsson orbitals are essential.

III. THE SIDEBANDS

Measurement of several sidebands is also reported in Ref. [1]. It is a crucial test for a microscopic theory of whether these bands are simultaneously reproduced as well. There can be two types of negative parity bands at lower excitation: neutron 2-qp bands based on one quasineutron from the ma-
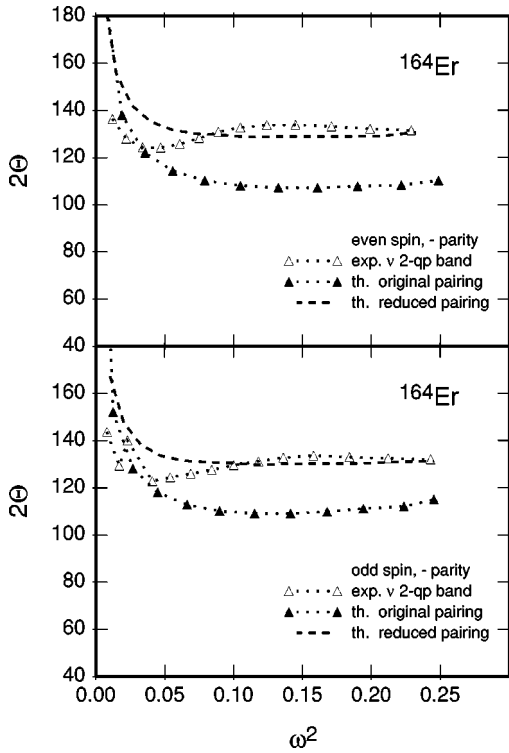
FIG. 3. Backbending plot for the neutron negative parity band (labeled as AE and AF in Ref. [1]) in ^{164}Er. The experimental data [1] are compared with two theoretical calculations. In both calculations, the Nilsson parameters in $N=5$ proton shell are multiplied by a factor 1.1. The filled triangles represent the results with the same pairing force strength used in the calculations for the positive parity bands. The dashed lines are the results with a reduced pairing strength (for the purpose of comparison only).

jor shell $N=5$ and another from $N=6$ as well as proton 2-qp bands based on one quasiproton from $N=4$ and another from $N=5$. At higher spins, the neutron 2-qp bands will be crossed by 4-qp bands built upon these neutron 2-qp states plus a quasiproton (positive parity) pair, while the proton 2-qp bands will be crossed by 4-qp bands built upon these proton 2-qp states plus a quasineutron (positive parity) pair. From the above discussions of the yrast band, the qp pairs in question are from the neutron $i_{13/2}$ and proton $h_{11/2}$ subshells.

In Fig. 3, the experimental data of the negative parity bands (labeled as AE and AF in Ref. [1]) are plotted as open triangles. The data are compared with the theoretical calculation presented as filled triangles. The calculation is done by using the Nilsson parameters with the same modifications for the $N=5$ proton shell. Namely, these results are obtained by using the same deformed single-particle basis and the same Hamiltonian as used for the filled circles in Fig. 1. The filled triangles shown here are the results after the band mixing with the major contribution from the neutron 2-qp state $i_{13/2}[\frac{5}{2}^+]\oplus h_{9/2}[\frac{5}{2}^-]$ ($K^\pi=5^-$). It is seen that the calculation agrees well with the first several points for both of the even and odd spin members, but a departure begins at $\omega^2\approx0.05$. A nearly constant deviation of about 20 MeV^{-1} (or 15% too small in theory) in the (two times of) moment of inertia plot is seen over the higher spin states. To improve the agreement, one needs a reduction factor of 0.92 in the (neutron and proton) pairing if one does not change anything else in
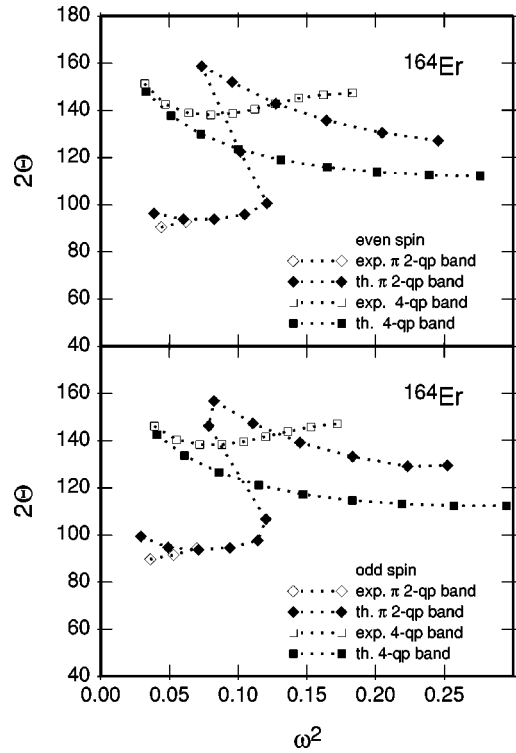
FIG. 4. Backbending plot for the proton negative parity band (labeled as $[7^-]$ in Ref. [1]) and the 4-qp band in ^{164}Er. The experimental data [1] are compared with the present theoretical calculations.

the calculation. These results are shown in Fig. 3 as dashed lines. This is unfortunate for the theory since we expect that all the states should come out correctly by a single diagonalization.

However, we emphasize here the necessity of the same modification in the Nilsson parameters for the $N=5$ proton shell. Without this modification, a backbending in the moment of inertia for both even- and odd-spin sequences would occur at $\omega^2\approx0.20$, which is not supported by the data. This unexpected backbending is independent of whether the pairing strength is reduced or not. It is understandable because the backbending is caused by a sharp band crossing of the 2-quasineutron band $i_{13/2}[\frac{5}{2}^+]\oplus h_{9/2}[\frac{5}{2}^-]$ with a 4-qp band built by this 2-quasineutron state plus an $h_{11/2}$ proton pair $[\frac{5}{2},-\frac{7}{2}]$ and this is the same mechanism why the unexpected second backbending appeared in the yrast band as discussed in Fig. 1. With the modification of the Nilsson parameters for the $N=5$ proton shell, this 4-qp band is pushed higher in energy and thus the undesired backbending is avoided.

The other type of negative parity bands is based on the proton 2-qp states. These 2-qp bands will be crossed by 4-qp bands which consist of the same 2-quasiproton states plus a pair of $i_{13/2}$ neutrons. In Fig. 4, we present results obtained by mixing these configurations. It is found that the lowest states at each spin show a similar backbending pattern as in the yrast band shown in Fig. 1. The major contribution to this band is from the 2-quasiproton state of $h_{11/2}[\frac{7}{2}^-]\oplus g_{9/2}[\frac{7}{2}^+]$ ($K^\pi=7^-$) before the band crossing and this 2-quasiproton state plus a neutron pair from the $i_{13/2}$ subshell (which can be a mixture of the three neutron pairs shown in
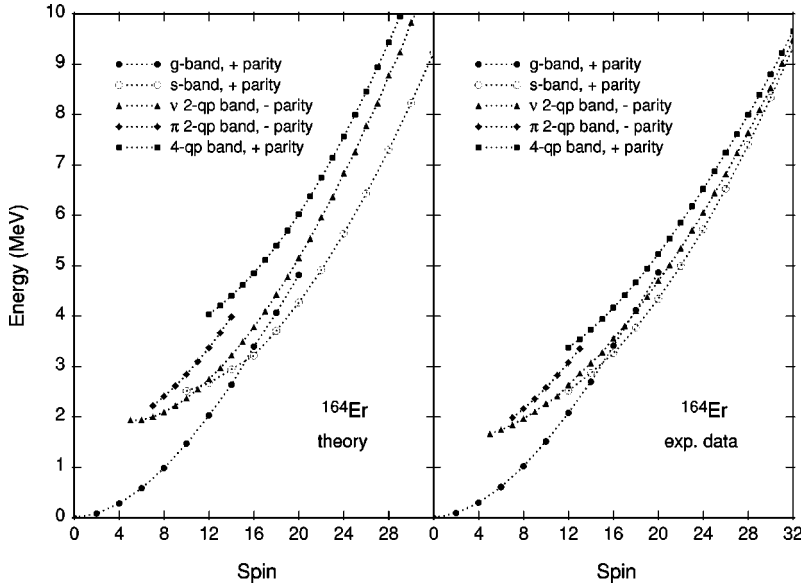
FIG. 5. Comparison of the PSM calculation (left) with all measured bands of Ref. [1] (right) for ^{164}Er in the excitation energy vs spin plot. Symbols used for each band are identical with those in the previous figures so that one can see the position of each excited band. Note that all bands shown in this figure are obtained from the same Hamiltonian with the modified proton $N=5$ shell spin-orbit parameters (but no modification of the pairing strength).

Fig. 2) after the crossing. For this band, the present experimental data (labeled as [7^-] in Ref. [1]) extend only over a few transitions. However, they agree rather well with our theory (see Fig. 4). Our prediction for the higher spin states may be eventually tested by possible extensions of this band by a future measurement.

As to the positive parity 4-qp band, we have constructed the 4-qp states from the two types of negative parity 2-qp states, one from neutron 2-qp and another from proton 2-qp states. The present calculation shows that, among this kind of configurations, a band based on $\nu i_{13/2}[\frac{5}{2}^+]\oplus h_{9/2}[\frac{5}{2}^-]$ and $\pi h_{11/2}[\frac{7}{2}^-]\oplus g_{9/2}[\frac{7}{2}^+]$ coupled totally to $K^\pi=12^+$ is really the lowest in energy and this supports the assignment suggested by Ref. [1]. In fact, the agreement of our calculation with the data is good at the beginning of the band as one can see in Fig. 4, although deviation becomes larger and larger at higher spins. Changing the pairing strength (as we did for Fig. 3) can hardly improve this result.

IV. SUMMARY

To summarize, we present all results of the PSM calculation and compare them with the experimental ones [1] in Fig. 5. It should be remarked that the theory uses the same Hamiltonian (with the modified proton $N=5$ Nilsson parameters as mentioned above) for all bands so that the whole set of states (at each spin) are obtained by a single diagonalization. The agreement is not perfect but satisfactory in the sense that one can understand the experimental data in a unified way from the PSM point of view. In fact, the theory describes the g-, s- (AB) and the proton 2-qp ([7^-]) bands very well for the entire spin region. The prediction for the states near the bandhead of the negative parity neutron 2-qp

band (AE and AF) is also fine but deviation develops for higher spin states. The result climbs up too fast and this is the reason why we get too small moment of inertia so far as the pairing is not modified (cf. Fig. 3). The theoretical result for the 4-qp band also deviates from the data roughly by a constant amount of 600 keV for the entire band. To cure these discrepancies, we would need an investigation of a larger scope than the present one.

Finally, we should like to call the readers attention to the crucial role of the Nilsson (spin-orbit) parameters whose quality is important, sometimes essential, for a correct theoretical description of the high-spin structure. For the nucleus ^{164}Er, the standard κ and μ lead to the occurrence of a second backbending in the yrast band and of a backbending in the negative parity neutron 2-qp band, both of which are not supported by the latest data. The effect of our simple-minded modification in the Nilsson parameters can be clearly seen in the present calculation. With the same modification for the $N=5$ proton shell, we have systematically tested all even-even nuclei calculated in our earlier paper Ref. [7] and found that the present modification does not destroy the achieved agreement with the data for Yb and Hf isotopes. On the other hand, the predicted weak second upbending in ^{166}Er and ^{168}Er [7] is gone in this new calculation, which is awaiting a future experimental verification. We have not confirmed whether or not this modification is compatible with other (i.e., odd-proton and odd-odd) types of nuclei. This will be done eventually. However, in light of today's quality and richness of high-spin data, the present result surely suggests the necessity of a systematic restudy of the Nilsson single-particle scheme, which is the starting point of many theoretical models, particularly of the projected shell model on which the present calculation is based.

[1] R. A. Bark *et al.*, Z. Phys. A **359**, 5 (1997).

[2] A. Johnson, H. Ryde, and J. Sztarkier, Phys. Lett. **34B**, 605 (1971).

[3] A. Johnson, H. Ryde, and S. A. Hjorth, Nucl. Phys. **A179**, 753 (1972).

[4] F. S. Stephens and R. S. Simon, Nucl. Phys. **A183**, 257 (1972).

[5] I. Y. Lee *et al.*, Phys. Rev. Lett. **37**, 420 (1976).

[6] O. C. Kistner, A. W. Sunyar, and E. der Mateosian, Phys. Rev. C **17**, 1417 (1978).

[7] K. Hara and Y. Sun, Nucl. Phys. **A529**, 445 (1991).

[8] K. Hara and Y. Sun, Int. J. Mod. Phys. E **4**, 637 (1995).

[9] R. Bengtsson, S. Frauendorf, and F.-R. May, At. Data Nucl. Data Tables **35**, 15 (1986).

[10] S. G. Nilsson *et al.*, Nucl. Phys. **A131**, 1 (1969).

[11] T. Bengtsson and I. Ragnarsson, Nucl. Phys. **A436**, 14 (1985).

[12] J.-Y. Zhang, A. J. Larabee, and L. L. Riedinger, J. Phys. G **13**, L75 (1987).

[13] T. Seo, Z. Phys. A **324**, 43 (1986).